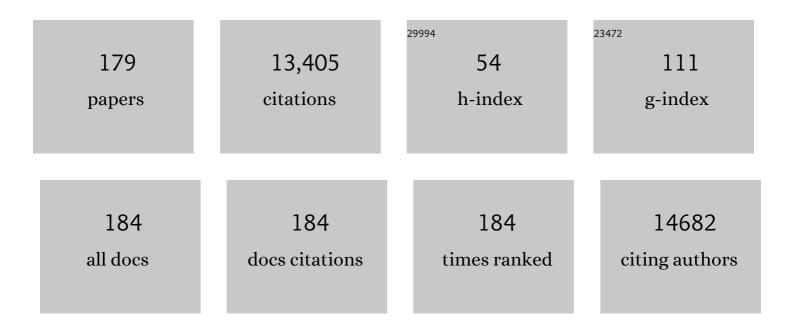


## List of Publications by Year in descending order

Source: https://exaly.com/author-pdf/539283/publications.pdf Version: 2024-02-01



WELLIO

#	Article	IF	CITATIONS
1	Carbon Electrodes for K-Ion Batteries. Journal of the American Chemical Society, 2015, 137, 11566-11569.	6.6	1,559
2	Self-Assembled Hierarchical MoO <sub>2</sub> /Graphene Nanoarchitectures and Their Application as a High-Performance Anode Material for Lithium-Ion Batteries. ACS Nano, 2011, 5, 7100-7107.	7.3	611
3	Heterogeneous Singleâ€Atom Catalysts for Electrochemical CO <sub>2</sub> Reduction Reaction. Advanced Materials, 2020, 32, e2001848.	11.1	366
4	Surface and Interface Engineering of Siliconâ€Based Anode Materials for Lithiumâ€lon Batteries. Advanced Energy Materials, 2017, 7, 1701083.	10.2	354
5	Amorphous TiO <sub>2</sub> Shells: A Vital Elastic Buffering Layer on Silicon Nanoparticles for Highâ€Performance and Safe Lithium Storage. Advanced Materials, 2017, 29, 1700523.	11.1	342
6	An Organic Pigment as a Highâ€Performance Cathode for Sodiumâ€Ion Batteries. Advanced Energy Materials, 2014, 4, 1400554.	10.2	339
7	Carbon nanofibers derived from cellulose nanofibers as a long-life anode material for rechargeable sodium-ion batteries. Journal of Materials Chemistry A, 2013, 1, 10662.	5.2	337
8	Sodium/Potassiumâ€ion Batteries: Boosting the Rate Capability and Cycle Life by Combining Morphology, Defect and Structure Engineering. Advanced Materials, 2020, 32, e1904320.	11.1	335
9	In-situ reconstructed Ru atom array on α-MnO2 with enhanced performance for acidic water oxidation. Nature Catalysis, 2021, 4, 1012-1023.	16.1	324
10	Pyrolysis of Cellulose under Ammonia Leads to Nitrogen-Doped Nanoporous Carbon Generated through Methane Formation. Nano Letters, 2014, 14, 2225-2229.	4.5	297
11	A Dualâ€Functional Conductive Framework Embedded with TiNâ€VN Heterostructures for Highly Efficient Polysulfide and Lithium Regulation toward Stable Li–S Full Batteries. Advanced Materials, 2020, 32, e1905658.	11.1	276
12	New Insight into the Synthesis of Large-Pore Ordered Mesoporous Materials. Journal of the American Chemical Society, 2017, 139, 1706-1713.	6.6	274
13	Highly Ordered Mesoporous Tungsten Oxides with a Large Pore Size and Crystalline Framework for H <sub>2</sub> S Sensing. Angewandte Chemie - International Edition, 2014, 53, 9035-9040.	7.2	250
14	Morphosynthesis of a hierarchical MoO2 nanoarchitecture as a binder-free anode for lithium-ion batteries. Energy and Environmental Science, 2011, 4, 2870.	15.6	245
15	Improved Thermoelectric Performance of Silver Nanoparticlesâ€Dispersed Bi <sub>2</sub> Te <sub>3</sub> Composites Deriving from Hierarchical Twoâ€Phased Heterostructure. Advanced Functional Materials, 2015, 25, 966-976.	7.8	243
16	An Interface Coassembly in Biliquid Phase: Toward Core–Shell Magnetic Mesoporous Silica Microspheres with Tunable Pore Size. Journal of the American Chemical Society, 2015, 137, 13282-13289.	6.6	239
17	Silicon/Mesoporous Carbon/Crystalline TiO <sub>2</sub> Nanoparticles for Highly Stable Lithium Storage. ACS Nano, 2016, 10, 10524-10532.	7.3	230
18	Low-Surface-Area Hard Carbon Anode for Na-Ion Batteries via Graphene Oxide as a Dehydration Agent. ACS Applied Materials & Interfaces, 2015, 7, 2626-2631.	4.0	226

#	Article	IF	CITATIONS
19	Engineering the Distribution of Carbon in Silicon Oxide Nanospheres at the Atomic Level for Highly Stable Anodes. Angewandte Chemie - International Edition, 2019, 58, 6669-6673.	7.2	209
20	Critical thickness of phenolic resin-based carbon interfacial layer for improving long cycling stability of silicon nanoparticle anodes. Nano Energy, 2016, 27, 255-264.	8.2	204
21	Electrochemically Expandable Soft Carbon as Anodes for Na-Ion Batteries. ACS Central Science, 2015, 1, 516-522.	5.3	202
22	Ultrafine MoO <sub>2</sub> nanoparticles embedded in a carbon matrix as a high-capacity and long-life anode for lithium-ion batteries. Journal of Materials Chemistry, 2012, 22, 425-431.	6.7	175
23	Synthesis of Ordered Mesoporous Silica with Tunable Morphologies and Pore Sizes via a Nonpolar Solvent-Assisted Stöber Method. Chemistry of Materials, 2016, 28, 2356-2362.	3.2	159
24	Ultrathin CoO/Graphene Hybrid Nanosheets: A Highly Stable Anode Material for Lithium-Ion Batteries. Journal of Physical Chemistry C, 2012, 116, 20794-20799.	1.5	154
25	A Micelle Fusion–Aggregation Assembly Approach to Mesoporous Carbon Materials with Rich Active Sites for Ultrasensitive Ammonia Sensing. Journal of the American Chemical Society, 2016, 138, 12586-12595.	6.6	152
26	Tailoring the Assembly of Iron Nanoparticles in Carbon Microspheres toward High-Performance Electrocatalytic Denitrification. Nano Letters, 2019, 19, 5423-5430.	4.5	147
27	Residual Chlorine Induced Cationic Active Species on a Porous Copper Electrocatalyst for Highly Stable Electrochemical CO <sub>2</sub> Reduction to C <sub>2+</sub> . Angewandte Chemie - International Edition, 2021, 60, 11487-11493.	7.2	145
28	Structure-based drug designing and immunoinformatics approach for SARS-CoV-2. Science Advances, 2020, 6, eabb8097.	4.7	138
29	Hollow-Carbon-Templated Few-Layered V <sub>5</sub> S <sub>8</sub> Nanosheets Enabling Ultrafast Potassium Storage and Long-Term Cycling. ACS Nano, 2019, 13, 7939-7948.	7.3	136
30	Efficient Fabrication of Nanoporous Si and Si/Ge Enabled by a Heat Scavenger in Magnesiothermic Reactions. Scientific Reports, 2013, 3, 2222.	1.6	125
31	Direct Superassemblies of Freestanding Metal–Carbon Frameworks Featuring Reversible Crystalline-Phase Transformation for Electrochemical Sodium Storage. Journal of the American Chemical Society, 2016, 138, 16533-16541.	6.6	120
32	Electrospinning of carbon-coated MoO2 nanofibers with enhanced lithium-storage properties. Physical Chemistry Chemical Physics, 2011, 13, 16735.	1.3	113
33	Two-dimensional hyperferroelectric metals: A different route to ferromagnetic-ferroelectric multiferroics. Physical Review B, 2017, 96, .	1.1	113
34	Ultrathin and Light-Weight Graphene Aerogel with Precisely Tunable Density for Highly Efficient Microwave Absorbing. ACS Applied Materials & Interfaces, 2019, 11, 46386-46396.	4.0	97
35	Chelation-assisted soft-template synthesis of ordered mesoporous zinc oxides for low concentration gas sensing. Journal of Materials Chemistry A, 2016, 4, 15064-15071.	5.2	93
36	Multi-layered mesoporous TiO <sub>2</sub> thin films with large pores and highly crystalline frameworks for efficient photoelectrochemical conversion. Journal of Materials Chemistry A, 2013, 1, 1591-1599.	5.2	91

#	Article	IF	CITATIONS
37	Ordered Mesoporous Alumina with Ultra-Large Pores as an Efficient Absorbent for Selective Bioenrichment. Chemistry of Materials, 2017, 29, 2211-2217.	3.2	89
38	A Resolâ€Assisted Coâ€Assembly Approach to Crystalline Mesoporous Niobia Spheres for Electrochemical Biosensing. Angewandte Chemie - International Edition, 2013, 52, 10505-10510.	7.2	85
39	Hierarchical Branched Mesoporous TiO <sub>2</sub> –SnO <sub>2</sub> Nanocomposites with Wellâ€Defined n–n Heterojunctions for Highly Efficient Ethanol Sensing. Advanced Science, 2019, 6, 1902008.	5.6	84
40	Boosting the initial coulombic efficiency in silicon anodes through interfacial incorporation of metal nanocrystals. Journal of Materials Chemistry A, 2019, 7, 17426-17434.	5.2	83
41	Boron doping-induced interconnected assembly approach for mesoporous silicon oxycarbide architecture. National Science Review, 2021, 8, nwaa152.	4.6	77
42	Mesoporous TiO <sub>2</sub> Mesocrystals: Remarkable Defects-Induced Crystallite-Interface Reactivity and Their in Situ Conversion to Single Crystals. ACS Central Science, 2015, 1, 400-408.	5.3	74
43	Amphiphilic Block Copolymer Templated Synthesis of Mesoporous Indium Oxides with Nanosheet-Assembled Pore Walls. Chemistry of Materials, 2016, 28, 7997-8005.	3.2	74
44	Rational Synthesis and Gas Sensing Performance of Ordered Mesoporous Semiconducting WO <sub>3</sub> /NiO Composites. ACS Applied Materials & Interfaces, 2019, 11, 26268-26276.	4.0	74
45	Dendritic Cellâ€Inspired Designed Architectures toward Highly Efficient Electrocatalysts for Nitrate Reduction Reaction. Small, 2020, 16, e2001775.	5.2	74
46	Performance of system consisting of vertical flow trickling filter and horizontal flow multi-soil-layering reactor for treatment of rural wastewater. Bioresource Technology, 2015, 193, 424-432.	4.8	70
47	Germanium Nanograin Decoration on Carbon Shell: Boosting Lithium‣torage Properties of Silicon Nanoparticles. Advanced Functional Materials, 2016, 26, 7800-7806.	7.8	68
48	Oxygen-deficient WO <sub>3â^'x</sub> @TiO <sub>2â^'x</sub> core–shell nanosheets for efficient photoelectrochemical oxidation of neutral water solutions. Journal of Materials Chemistry A, 2017, 5, 14697-14706.	5.2	68
49	Toward understanding the interaction within Silicon-based anodes for stable lithium storage. Chemical Engineering Journal, 2020, 385, 123821.	6.6	65
50	Controlled Synthesis of Ordered Mesoporous Carbon-Cobalt Oxide Nanocomposites with Large Mesopores and Graphitic Walls. Chemistry of Materials, 2016, 28, 7773-7780.	3.2	63
51	Silicon: toward eco-friendly reduction techniques for lithium-ion battery applications. Journal of Materials Chemistry A, 2019, 7, 24715-24737.	5.2	61
52	Surface modification of electrospun TiO2 nanofibers via layer-by-layer self-assembly for high-performance lithium-ion batteries. Journal of Materials Chemistry, 2012, 22, 4910.	6.7	60
53	Sub-nanometric Manganous Oxide Clusters in Nitrogen Doped Mesoporous Carbon Nanosheets for High-Performance Lithium–Sulfur Batteries. Nano Letters, 2021, 21, 700-708.	4.5	60
54	Enhancing the performance of Ce:YAG phosphor-in-silica-glass by controlling interface reaction. Acta Materialia, 2017, 130, 289-296.	3.8	58

#	Article	IF	CITATIONS
55	Bimetallic PdCu Nanocrystals Immobilized by Nitrogen-Containing Ordered Mesoporous Carbon for Electrocatalytic Denitrification. ACS Applied Materials & Interfaces, 2019, 11, 3861-3868.	4.0	57
56	When Silicon Materials Meet Natural Sources: Opportunities and Challenges for Lowâ€Cost Lithium Storage. Small, 2021, 17, e1904508.	5.2	56
57	Enhancing the Electrochemical Performance of Sodiumâ€lon Batteries by Building Optimized NiS <sub>2</sub> /NiSe <sub>2</sub> Heterostructures. Small, 2021, 17, e2104186.	5.2	56
58	Thin Film Thermoelectric Materials: Classification, Characterization, and Potential for Wearable Applications. Coatings, 2018, 8, 244.	1.2	54
59	Facile synthesis of one-dimensional peapod-like Sb@C submicron-structures. Chemical Communications, 2014, 50, 5435.	2.2	53
60	Modulating the Electronic Structure of FeCo Nanoparticles in Nâ€Đoped Mesoporous Carbon for Efficient Oxygen Reduction Reaction. Advanced Science, 2022, 9, e2200394.	5.6	52
61	Interface-Amorphized Ti <sub>3</sub> C <sub>2</sub> @Si/SiO <i><sub>x</sub></i> @TiO <sub>2</sub> Anodes with Sandwiched Structures and Stable Lithium Storage. ACS Applied Materials & Interfaces, 2020, 12, 24796-24805.	4.0	51
62	Conversion of Catalytically Inert 2D Bismuth Oxide Nanosheets for Effective Electrochemical Hydrogen Evolution Reaction Catalysis via Oxygen Vacancy Concentration Modulation. Nano-Micro Letters, 2022, 14, 90.	14.4	51
63	Hierarchical self-assembly of Mn2Mo3O8–graphene nanostructures and their enhanced lithium-storage properties. Journal of Materials Chemistry, 2011, 21, 17229.	6.7	50
64	Boron heteroatom-doped silicon–carbon peanut-like composites enables long life lithium-ion batteries. Rare Metals, 2022, 41, 1276-1283.	3.6	50
65	Monodisperse mesoporous TiO2 microspheres for dye sensitized solar cells. Nano Energy, 2016, 26, 16-25.	8.2	49
66	Mesoporous Materials–Based Electrochemical Biosensors from Enzymatic to Nonenzymatic. Small, 2021, 17, e1904022.	5.2	49
67	Highly dispersed Pt nanoparticles on ultrasmall EMT zeolite: A peroxidase-mimic nanoenzyme for detection of H2O2 or glucose. Journal of Colloid and Interface Science, 2020, 570, 300-311.	5.0	48
68	Improved Electrochemical Performance in Li3V2(PO4)3 Promoted by Niobium-Incorporation. Journal of the Electrochemical Society, 2011, 158, A924.	1.3	46
69	Carbon-Encapsulated Copper Sulfide Leading to Enhanced Thermoelectric Properties. ACS Applied Materials & Interfaces, 2019, 11, 22457-22463.	4.0	45
70	Constructing Structurally Ordered Highâ€Entropy Alloy Nanoparticles on Nitrogenâ€Rich Mesoporous Carbon Nanosheets for Highâ€Performance Oxygen Reduction. Advanced Materials, 2022, 34, e2110128.	11.1	44
71	Largeâ€Pore Mesoporous CeO <sub>2</sub> –ZrO <sub>2</sub> Solid Solutions with Inâ€Pore Confined Pt Nanoparticles for Enhanced CO Oxidation. Small, 2019, 15, e1903058.	5.2	43
72	Prediction of Silicon-Based Layered Structures for Optoelectronic Applications. Journal of the American Chemical Society, 2014, 136, 15992-15997.	6.6	42

#	Article	IF	CITATIONS
73	Tricomponent Coassembly Approach To Synthesize Ordered Mesoporous Carbon/Silica Nanocomposites and Their Derivative Mesoporous Silicas with Dual Porosities. Chemistry of Materials, 2014, 26, 2438-2444.	3.2	41
74	Unusual Ferroelectricity in Two-Dimensional Perovskite Oxide Thin Films. Nano Letters, 2018, 18, 595-601.	4.5	41
75	An Efficient Emulsionâ€Induced Interface Assembly Approach for Rational Synthesis of Mesoporous Carbon Spheres with Versatile Architectures. Advanced Functional Materials, 2020, 30, 2002488.	7.8	38
76	Mechanisms and strategies of microbial cometabolism in the degradation of organic compounds – chlorinated ethylenes as the model. Water Science and Technology, 2014, 69, 1971-1983.	1.2	37
77	Ordered mesoporous C/TiO <sub>2</sub> composites as advanced sonocatalysts. Journal of Materials Chemistry A, 2014, 2, 16452-16458.	5.2	37
78	Bowl-like mesoporous polymer-induced interface growth of molybdenum disulfide for stable lithium storage. Chemical Engineering Journal, 2020, 381, 122651.	6.6	37
79	Pushing the Limit of Ordered Mesoporous Materials via 2D Selfâ€Assembly for Energy Conversion and Storage. Advanced Functional Materials, 2021, 31, 2007496.	7.8	36
80	Twoâ€Đimensional Phosphorus Oxides as Energy and Information Materials. Angewandte Chemie - International Edition, 2016, 55, 8575-8580.	7.2	35
81	Pore Engineering of Mesoporous Tungsten Oxides for Ultrasensitive Gas Sensing. Advanced Materials Interfaces, 2019, 6, 1801269.	1.9	35
82	Chemical Vapor Deposition Mediated Phase Engineering for 2D Transition Metal Dichalcogenides: Strategies and Applications. Small Science, 2022, 2, 2100047.	5.8	35
83	A Universal Singleâ€Atom Coating Strategy Based on Tannic Acid Chemistry for Multifunctional Heterogeneous Catalysis. Angewandte Chemie - International Edition, 2022, 61, .	7.2	34
84	Facile synthesis of mesoporous WO3@graphene aerogel nanocomposites for low-temperature acetone sensing. Chinese Chemical Letters, 2019, 30, 2032-2038.	4.8	33
85	Ordered mesoporous CoO/CeO2 heterostructures with highly crystallized walls and enhanced peroxidase-like bioactivity. Applied Materials Today, 2019, 15, 482-493.	2.3	33
86	NiPt Nanocatalysts Supported on Boron and Nitrogen Coâ€Doped Graphene for Superior Hydrazine Dehydrogenation and Methanol Oxidation. ChemCatChem, 2016, 8, 1410-1416.	1.8	32
87	Mesoporous WO3 Nanofibers With Crystalline Framework for High-Performance Acetone Sensing. Frontiers in Chemistry, 2019, 7, 266.	1.8	32
88	Organic/Inorganic Hybrid Fibers: Controllable Architectures for Electrochemical Energy Applications. Advanced Science, 2021, 8, e2102859.	5.6	32
89	Highly Improved Microwave Absorbing and Mechanical Properties in Cold Sintered ZnO by Incorporating Graphene Oxide. Journal of the European Ceramic Society, 2022, 42, 993-1000.	2.8	31
90	Liquid Phase Interfacial Surface-Enhanced Raman Scattering Platform for Ratiometric Detection of MicroRNA 155. Analytical Chemistry, 2020, 92, 15573-15578.	3.2	29

#	Article	IF	CITATIONS
91	Revealing the superlative electrochemical properties of o-B2N2 monolayer in Lithium/Sodium-ion batteries. Nano Energy, 2022, 96, 107066.	8.2	29
92	A Robust Hierarchical MXene/Ni/Aluminosilicate Glass Composite for Highâ€Performance Microwave Absorption. Advanced Science, 2022, 9, e2104163.	5.6	29
93	Hierarchical ordered macro/mesoporous titania with a highly interconnected porous structure for efficient photocatalysis. Journal of Materials Chemistry A, 2016, 4, 16446-16453.	5.2	27
94	CT/NIRF dual-modal imaging tracking and therapeutic efficacy of transplanted mesenchymal stem cells labeled with Au nanoparticles in silica-induced pulmonary fibrosis. Journal of Materials Chemistry B, 2020, 8, 1713-1727.	2.9	27
95	Fluoride ion batteries: Designing flexible M2CH2 (M=Ti or V) MXenes as high-capacity cathode materials. Nano Energy, 2020, 74, 104911.	8.2	27
96	A confined micro-reactor with a movable Fe3O4 core and a mesoporous TiO2 shell for a photocatalytic Fenton-like degradation of bisphenol A. Chinese Chemical Letters, 2021, 32, 1456-1461.	4.8	27
97	Third-order nonlinear optical vitreous material derived from mesoporous silica incorporated with Au nanoparticles. Journal of Materials Chemistry C, 2014, 2, 6966-6970.	2.7	25
98	Copper thiocyanate/copper iodide based hole transport composites with balanced properties for efficient polymer light-emitting diodes. Journal of Materials Chemistry C, 2018, 6, 4895-4902.	2.7	25
99	Big Potential From Silicon-Based Porous Nanomaterials: In Field of Energy Storage and Sensors. Frontiers in Chemistry, 2018, 6, 539.	1.8	24
100	Interface Heteroatomâ€doping: Emerging Solutions to Siliconâ€based Anodes. Chemistry - an Asian Journal, 2020, 15, 1394-1404.	1.7	24
101	Production of graphene by reduction using a magnesiothermic reaction. Chemical Communications, 2013, 49, 10676.	2.2	23
102	Quantified mass transfer and superior antiflooding performance of ordered macroâ€mesoporous electrocatalysts. AICHE Journal, 2018, 64, 2881-2889.	1.8	22
103	Controllable synthesis of highly crystallized mesoporous TiO2/WO3 heterojunctions for acetone gas sensing. Chinese Chemical Letters, 2020, 31, 1119-1123.	4.8	22
104	High-capacity reversible hydrogen storage properties of metal-decorated nitrogenated holey graphenes. International Journal of Hydrogen Energy, 2022, 47, 10654-10664.	3.8	22
105	Structural prediction of host-guest structure in lithium at high pressure. Scientific Reports, 2018, 8, 5278.	1.6	21
106	Variants in Homologous Recombination Genes <i>EXO1</i> and <i>RAD51</i> Related with Premature Ovarian Insufficiency. Journal of Clinical Endocrinology and Metabolism, 2020, 105, e3566-e3574.	1.8	21
107	Sinterability Enhancement by Collapse of Mesoporous Structure of <scp>SBA</scp> â€15 in Fabrication of Highly Transparent Silica Glass. Journal of the American Ceramic Society, 2015, 98, 1056-1059.	1.9	20
108	Ambient hydrolysis deposition of TiO2 in nanoporous carbon and the converted TiN–carbon capacitive electrode. Journal of Materials Chemistry A, 2014, 2, 2901.	5.2	19

#	Article	IF	CITATIONS
109	Emulsion-templated poly(acrylamide)s by using polyvinyl alcohol (PVA) stabilized CO <sub>2</sub> -in-water emulsions and their applications in tissue engineering scaffolds. RSC Advances, 2015, 5, 92017-92024.	1.7	19
110	Enhanced butanol production by solvent tolerance Clostridium acetobutylicum SE25 from cassava flour in a fibrous bed bioreactor. Bioresource Technology, 2016, 221, 412-418.	4.8	19
111	Spatially Confined Tuning the Interfacial Synergistic Catalysis in Mesochannels toward Selective Catalytic Reduction. ACS Applied Materials & amp; Interfaces, 2019, 11, 19242-19251.	4.0	19
112	Ground–state structure of semiconducting and superconducting phases in xenon carbides at high pressure. Scientific Reports, 2019, 9, 2459.	1.6	19
113	Ramie-degumming methodologies: A short review. Journal of Engineered Fibers and Fabrics, 2020, 15, 155892502094010.	0.5	18
114	Properties of MgO transparent ceramics prepared at low temperature using high sintering activity MgO powders. Journal of the American Ceramic Society, 2020, 103, 5382-5391.	1.9	18
115	Amphiphilic block copolymers directed synthesis of mesoporous nickel-based oxides with bimodal mesopores and nanocrystal-assembled walls. Chinese Chemical Letters, 2019, 30, 2003-2008.	4.8	17
116	Stepwise construction of Pt decorated oxygen-deficient mesoporous titania microspheres with core-shell structure and magnetic separability for efficient visible-light photocatalysis. Chinese Chemical Letters, 2020, 31, 1598-1602.	4.8	17
117	Cloning and Expression of a Novel Leucine Dehydrogenase: Characterization and L-tert-Leucine Production. Frontiers in Bioengineering and Biotechnology, 2020, 8, 186.	2.0	17
118	Incorporating Cobalt Nanoparticles in Nitrogen-Doped Mesoporous Carbon Spheres through Composite Micelle Assembly for High-Performance Lithium–Sulfur Batteries. ACS Applied Materials & Interfaces, 2021, 13, 38604-38612.	4.0	17
119	Formation and electronic properties of palladium hydrides and palladium-rhodium dihydride alloys under pressure. Scientific Reports, 2017, 7, 3520.	1.6	16
120	The High-Pressure Superconducting Phase of Arsenic. Scientific Reports, 2018, 8, 3026.	1.6	16
121	Crude glycerol from biodiesel as a carbon source for production of a recombinant highly thermostable β-mannanase by Pichia pastoris. Biotechnology Letters, 2018, 40, 135-141.	1.1	16
122	Engineering the Distribution of Carbon in Silicon Oxide Nanospheres at the Atomic Level for Highly Stable Anodes. Angewandte Chemie, 2019, 131, 6741-6745.	1.6	16
123	Red Phosphorus Anchored on Nitrogenâ€Doped Carbon Bubbleâ€Carbon Nanotube Network for Highly Stable and Fastâ€Charging Lithiumâ€lon Batteries. Small, 2022, 18, e2105866.	5.2	16
124	Porous arbon onfined Formation of Monodisperse Iron Nanoparticle Yolks toward Versatile Nanoreactors for Metal Extraction. Chemistry - A European Journal, 2018, 24, 15663-15668.	1.7	15
125	Confined interfacial micelle aggregating assembly of ordered macro–mesoporous tungsten oxides for H <sub>2</sub> S sensing. Nanoscale, 2020, 12, 20811-20819.	2.8	15
126	Residual Chlorine Induced Cationic Active Species on a Porous Copper Electrocatalyst for Highly Stable Electrochemical CO 2 Reduction to C 2+. Angewandte Chemie, 2021, 133, 11588-11594.	1.6	15

#	Article	IF	CITATIONS
127	B-incorporated, N-doped hierarchically porous carbon nanosheets as anodes for boosted potassium storage capability. Chinese Chemical Letters, 2022, 33, 480-485.	4.8	15
128	Comparison of Additives in Anode: The Case of Graphene, MXene, CNTs Integration with Silicon Inside Carbon Nanofibers. Acta Metallurgica Sinica (English Letters), 2021, 34, 337-346.	1.5	14
129	N 1-{4-[(10S)-Dihydroartemisinin-10-oxyl]}phenylmethylene-N 2-(2-methylquinoline-4-yl)hydrazine derivatives as antiplasmodial falcipain-2 inhibitors. Medicinal Chemistry Research, 2012, 21, 3073-3079.	1.1	13
130	Cobalt-based magnetic Weyl semimetals with high-thermodynamic stabilities. Npj Computational Materials, 2021, 7, .	3.5	13
131	Interfacial engineering of core-shell structured mesoporous architectures from single-micelle building blocks. Nano Today, 2020, 35, 100940.	6.2	12
132	Enhancement in sintering driving force derived from in situ ordered structural collapse of mesoporous powders. Journal of the American Ceramic Society, 2020, 103, 5654-5663.	1.9	12
133	Enriching Atomic Cobalt in an Ultrathin Porous Carbon Shell for Enhanced Electrocatalysis. ACS Applied Materials & Interfaces, 2021, 13, 52167-52173.	4.0	12
134	Enhanced production of l-tryptophan with glucose feeding and surfactant addition and related metabolic flux redistribution in the recombinant Escherichia coli. Food Science and Biotechnology, 2013, 22, 207-214.	1.2	11
135	Solidâ€ <del>S</del> tate Sintering of Glasses with Optical Nonlinearity from Mesoporous Powders. Journal of the American Ceramic Society, 2016, 99, 1579-1586.	1.9	11
136	Nearâ€Infrared Broadband Photoluminescence of Bismuthâ€Doped Zeoliteâ€Derived Silica Glass Prepared by <scp>SPS</scp> . Journal of the American Ceramic Society, 2016, 99, 121-127.	1.9	11
137	Yolk-shell structured Fe@void@mesoporous silica with high magnetization for activating peroxymonosulfate. Chinese Chemical Letters, 2020, 31, 2003-2006.	4.8	11
138	Liquidâ€Phase Assisted Engineering of Highly Strong SiC Composite Reinforced by Multiwalled Carbon Nanotubes. Advanced Science, 2020, 7, 2002225.	5.6	11
139	Impulsive Synchronization of Fractional-Order Chaotic Systems With Actuator Saturation and Control Gain Error. IEEE Access, 2020, 8, 36113-36119.	2.6	11
140	A facile biliquid-interface co-assembly synthesis of mesoporous vesicles with large pore sizes. CrystEngComm, 2016, 18, 4343-4348.	1.3	10
141	Regulating ambient pressure approach to graphitic carbon nitride towards dispersive layers and rich pyridinic nitrogen. Chinese Chemical Letters, 2020, 31, 1603-1607.	4.8	10
142	A Negative Regulator of Carotenogenesis in <i>Blakeslea trispora</i> . Applied and Environmental Microbiology, 2020, 86, .	1.4	10
143	Phase engineering of dual active 2D Bi <sub>2</sub> O <sub>3</sub> -based nanocatalysts for alkaline hydrogen evolution reaction electrocatalysis. Journal of Materials Chemistry A, 2022, 10, 808-817.	5.2	10
144	A Universal Singleâ€Atom Coating Strategy Based on Tannic Acid Chemistry for Multifunctional Heterogeneous Catalysis. Angewandte Chemie, 2022, 134, .	1.6	9

#	Article	IF	CITATIONS
145	Controlled PEGylation of periodic mesoporous organosilica nanospheres for improving their stability in physiological solutions. Chinese Chemical Letters, 2019, 30, 929-932.	4.8	8
146	Lowâ€Dimensional Copper Selenide Nanostructures: Controllable Morphology and its Dependence on Electrocatalytic Performance. ChemElectroChem, 2019, 6, 574-580.	1.7	8
147	Two-dimensional topological semimetals protected by symmorphic symmetries. Physical Review B, 2020, 101, .	1.1	8
148	Biodegradation of Acetochlor by a Newly Isolated Pseudomonas Strain. Applied Biochemistry and Biotechnology, 2015, 176, 636-644.	1.4	7
149	Solution-phase synthesis of ordered mesoporous carbon as resonant-gravimetric sensing material for room-temperature H2S detection. Chinese Chemical Letters, 2020, 31, 1680-1685.	4.8	7
150	Ordered mesoporous carbon-silica frameworks confined magnetic mesoporous TiO2 as an efficient catalyst under acoustic cavitation energy. Journal of Materiomics, 2020, 6, 45-53.	2.8	7
151	Recent advances on the synthesis of mesoporous metals for electrocatalytic methanol oxidation. Emergent Materials, 2020, 3, 291-306.	3.2	7
152	Blakeslea trispora Photoreceptors: Identification and Functional Analysis. Applied and Environmental Microbiology, 2020, 86, .	1.4	7
153	Screening and identification of pectinolytic bacteria for ramie degumming. Textile Reseach Journal, 2021, 91, 1056-1064.	1.1	7
154	Genetic algorithm prediction of pressure-induced multiferroicity in the perovskite <mml:math xmlns:mml="http://www.w3.org/1998/Math/MathML"><mml:mrow><mml:mi>PbCo</mml:mi><mml:msub><mml:mathvariant="normal">O<mml:mn>3</mml:mn></mml:mathvariant="normal"></mml:msub></mml:mrow></mml:math> . Physical Review B, 2019, 99, .	mi 1 <b>.</b> 1	6
155	A Unique ATPase, ArtR (PA4595), Represses the Type III Secretion System in Pseudomonas aeruginosa. Frontiers in Microbiology, 2019, 10, 560.	1.5	6
156	A novel FOXL2 mutation in two infertile patients with blepharophimosis–ptosis–epicanthus inversus syndrome. Journal of Assisted Reproduction and Genetics, 2020, 37, 223-229.	1.2	6
157	Ultraâ€low temperature preparation of mullite glassâ€ceramics with high transparency sintered from EMTâ€type zeolite. Journal of the American Ceramic Society, 2021, 104, 3158-3166.	1.9	6
158	Oriented assembly of monomicelles in beam stream enabling bimodal mesoporous metal oxide nanofibers. Science China Materials, 2021, 64, 2486-2496.	3.5	6
159	Electrostatic Interactions Leading to Hierarchical Interpenetrating Electroconductive Networks in Silicon Anodes for Fast Lithium Storage. Chemistry - A European Journal, 2021, 27, 9320-9327.	1.7	6
160	Multilevel Regulation of Carotenoid Synthesis by Light and Active Oxygen in <i>Blakeslea trispora</i> . Journal of Agricultural and Food Chemistry, 2021, 69, 10974-10988.	2.4	6
161	Polydopamine-Derived Carbon: What a Critical Role for Lithium Storage?. Frontiers in Energy Research, 2020, 8, .	1.2	5
162	General Cutting Load Model for Workload Simulation in Spindle Reliability Test. Machines, 2022, 10, 144.	1.2	5

#	Article	IF	CITATIONS
163	In-Situ Reduction of Mo-Based Composite Particles during Laser Powder Bed Fusion. Crystals, 2021, 11, 702.	1.0	4
164	Synthesis of L-asparagine Catalyzed by a Novel Asparagine Synthase Coupled With an ATP Regeneration System. Frontiers in Bioengineering and Biotechnology, 2021, 9, 747404.	2.0	4
165	Floquet band engineering and topological phase transitions in 1T' transition metal dichalcogenides. 2D Materials, 2022, 9, 025005.	2.0	4
166	The nonlinear optical properties of silver nanoparticles decorated glass obtained from sintering mesoporous powders. Journal of the American Ceramic Society, 2021, 104, 2571-2578.	1.9	3
167	A Comprehensive Review of Permanent Magnet Synchronous Linear Motors in automotive electromagnetic suspension system. , 2021, , .		3
168	Highly Efficient Oxygenâ€Modulated Ruâ€Based HER Electrocatalyst in a Wide pH Range. ChemElectroChem, 2022, 9, .	1.7	3
169	Highly ordered mesoporous 1T' MoTe2/m-SiO2 composite as efficient microwave absorber. Microporous and Mesoporous Materials, 2022, , 111894.	2.2	3
170	Synthesis and evaluation in vitro of 1-[2-(10-dihydroartemisininoxy) ethyl]-3-phenylurea derivatives as potential agents against cancer. Medicinal Chemistry Research, 2013, 22, 3170-3176.	1.1	2
171	Comparative Analysis Among Different Species Reveals That the Androgen Receptor Regulates Chicken Follicle Selection Through Species-Specific Genes Related to Follicle Development. Frontiers in Genetics, 2021, 12, 752976.	1.1	2
172	Self-organization of unimolecular micelles in beam stream for functional mesoporous metal oxide nanofibers. Fundamental Research, 2022, 2, 776-782.	1.6	2
173	Study of Oleophobic Modification of Fiber Material Surface and Its Performance. Fibers and Polymers, 2019, 20, 1145-1154.	1.1	1
174	An Adaptive Bayesian Melding Method for Reliability Evaluation Via Limited Failure Data: An Application to the Servo Turret. Applied Sciences (Switzerland), 2020, 10, 7591.	1.3	1
175	A carbon network strategy to synthesize silicon–carbon anodes toward regulated morphologies during molten salt reduction. CrystEngComm, 2020, 22, 4894-4902.	1.3	1
176	Atomistic Site Control of Pd in Crystalline MnO <sub>2</sub> Nanofiber for Enhanced Electrocatalysis. Advanced Materials Interfaces, 2021, 8, 2002060.	1.9	1
177	Classification method of production system equipment importance based on grey correlation interval AHP-Entropy method. Journal of Advanced Mechanical Design, Systems and Manufacturing, 2020, 14, JAMDSM0094-JAMDSM0094.	0.3	1
178	Nanoparticles: Germanium Nanograin Decoration on Carbon Shell: Boosting Lithium-Storage Properties of Silicon Nanoparticles (Adv. Funct. Mater. 43/2016). Advanced Functional Materials, 2016, 26, 7799-7799.	7.8	0
179	Research on Sensitive Measuring Points for Vibration Fault of NC Turret Based on Energy Flow and Transfer Path. Mathematical Problems in Engineering, 2021, 2021, 1-16.	0.6	0